dered model, with a maximum dimension of 2.2 km, is consistent with those authors' statement that the illuminated, visible area had a maximum size "most likely in the range from 1.7 to 2.4 km." Noll *et al.* also interpreted the HST data as suggesting an "extended feature at an angle of about 45° off the solar vector," which is indicated by the line in Fig. 4C. This apparent elongation was the result of the unusual shape of Toutatis and shadowing effects arising from the large illumination angle.

All of Toutatis's surface was observed in the 18-day sequence of images (*11*), and because of the NPA rotation, the entire inertia tensor can be determined to within a constant factor. The dynamical penalties that forced the shape and inertia tensor toward mutual consistency with uniform density were exerting negligible pressure on the best-fit solution; removing them led to no significant change in the model. That is, the model requires either that Toutatis is nearly homogeneous or that its inhomogeneities mimic the inertia tensor of a homogeneous body (*12*).

The source of Toutatis's topographic bifurcation is a mystery. Might feature N have been sculpted by a single direct impact or a sequence of impacts? Or is Toutatis a contact binary formed in a gentle collision between L1 and L2? One would also like to decipher the collisional history responsible for the R1-R2-R3 structure, as well as implications of the global topography at all perceptible scales for the object's internal configuration, for example, its cohesiveness (*13*). One is especially interested in how and when Toutatis was excited into such a slow, NPA rotation state (*14*). Collisional simulations (*15*) using our physical model may suggest answers to these questions.

REFERENCES AND NOTES

1. S. J. Ostro *et al.*, *Science* **270**, 80 (1995).
2. R. S. Hudson and S. J. Ostro, *ibid.* **263**, 940 (1994).
3. L. D. Landau and E. M. Lifshitz, *Mechanics* (Pergamon, New York, 1976); N. H. Samarasinha and M. F. A'Hearn, *Icarus* **93**, 194 (1991); M. J. S. Belton, W. H. Julian, A. J. Anderson, B. E. A. Mueller, *ibid.*, p. 183.
4. The differential radar cross section of the surface was modeled as $\sigma_0 = \rho\cos^n i$ (*2*). The model yielded the value $n = 2.3 \pm 0.5$; $n = 2$ corresponds to Lambertian scattering, or a "perfectly rough" surface.
5. D. Hearn and M. P. Baker, *Computer Graphics* (Prentice Hall, Englewood Cliffs, NJ, ed. 2, 1994).
6. These define an effective diameter of 2.45 km. Thermal modeling by various researchers had suggested effective diameters between 2 and 3 km. D. J. Tholen, *Bull. Am. Astron. Soc.* **24**, 934 (1992); D. F. Lupishko, S. V. Vasilyev, J. S. Efimov, N. M. Shakhovskoj, *Icarus* **113**, 200 (1995).
7. S. J. Ostro *et al.*, *Nature* **375**, 474 (1995).
8. J. R. Spencer *et al.* [*Icarus*, in press] attempted to deduce the spin period of Toutatis from optical light curves. They found a best fit for $P = 7.25$ days but concluded from the poor fit that the rotation was more complex than PA.
9. I. de Pater *et al.*, *Icarus* **111**, 489 (1994).
10. K. S. Noll, H. A. Weaver, A. D. Storrs, B. Zellner, *ibid.* **113**, 353 (1995).
11. This was not apparent until the modeling was completed.
12. All detailed asteroid shape modeling to date has failed to find evidence for significant inhomogeneity (*2*); P. C. Thomas *et al.*, *Icarus* **107**, 23 (1994); P. C. Thomas *et al.*, *ibid.*, in press.
13. W. F. Bottke Jr. and J. J. Melosh, *Proc. Lunar Planet Sci. Conf.* **26**, 153 (1995).
14. A. W. Harris, *Icarus* **107**, 209 (1994); J. A. Burns and V. S. Safronov, *Mon. Not. R. Astron. Soc.* **165**, 403 (1973).
15. E. Asphaug *et al.*, *Icarus*, in press.

16. Part of this research was conducted at the Jet Propulsion Laboratory, California Institute of Technology, under contract with the National Aeronautics and Space Administration (NASA). Work at Washington State University was supported in part by NASA.

5 May 1995; accepted 14 August 1995

Myt1: A Membrane-Associated Inhibitory Kinase That Phosphorylates Cdc2 on Both Threonine-14 and Tyrosine-15

Paul R. Mueller, Thomas R. Coleman, Akiko Kumagai, William G. Dunphy*

Cdc2 is the cyclin-dependent kinase that controls entry of cells into mitosis. Phosphorylation of Cdc2 on threonine-14 and tyrosine-15 inhibits the activity of the enzyme and prevents premature initiation of mitosis. Although Wee1 has been identified as the kinase that phosphorylates tyrosine-15 in various organisms, the threonine-14–specific kinase has not been isolated. A complementary DNA was cloned from *Xenopus* that encodes Myt1, a member of the Wee1 family that was discovered to phosphorylate Cdc2 efficiently on both threonine-14 and tyrosine-15. Myt1 is a membrane-associated protein that contains a putative transmembrane segment. Immunodepletion studies suggested that Myt1 is the predominant threonine-14–specific kinase in *Xenopus* egg extracts. Myt1 activity is highly regulated during the cell cycle, suggesting that this relative of Wee1 plays a role in mitotic control.

Entry into mitosis is controlled by the M phase–promoting factor (MPF), a complex of the Cdc2 protein kinase and cyclin B. Proper regulation of MPF ensures that mitosis occurs only after earlier phases of the cell cycle have been completed successfully. This strict control of MPF is largely post-translational, involving the phosphorylation of Cdc2 at three key residues. After Cdc2 associates with cyclin, the cyclin-dependent kinase (CDK)–activating kinase (CAK) phosphorylates Cdc2 on Thr^{161}. This phosphorylation would generate active MPF, but two additional phosphorylations on Thr^{14} and Tyr^{15} of Cdc2 suppress MPF activity during interphase. At the G_2-M transition, the Cdc25 protein dephosphorylates Thr^{14} and Tyr^{15}, thereby allowing MPF to phosphorylate its mitotic substrates (*1*).

Various genetic and biochemical studies have indicated that Wee1 is the kinase that phosphorylates Cdc2 on Tyr^{15}. Wee1 was originally identified in the fission yeast *Schizosaccharomyces pombe* as a critical negative regulator of mitosis (*2*). Subsequently, a second *S. pombe* homolog (Mik1) and Wee1 homologs from at least six other organisms have been found (*3*, *4*). In human and *Xenopus*, Wee1 is a soluble enzyme that phosphorylates Cdc2 on Tyr^{15}, but not on Thr^{14} (*4*–*6*). A Thr^{14}-specific kinase activity has been detected in the membrane fraction of *Xenopus* egg extracts, but the molecular identity of the enzyme has not been established (*7*).

Previously we isolated a *Xenopus* Wee1 homolog. We used degenerate polymerase chain reaction (PCR) primers (based on the sequence similarity between *S. pombe* Wee1, *S. pombe* Mik1, and human Wee1) to amplify a segment of its complementary DNA (cDNA) (*4*). With a different combination of primers, we have amplified a segment of another *Xenopus* oocyte cDNA that appears to encode a distinct member of the Wee1 family. After cloning the corresponding full-length cDNA and characterizing its gene product (Fig. 1A), we designated this protein Myt1 for the membrane-associated, tyrosine- and threonine-specific, Cdc2 inhibitory kinase.

Conceptual translation of the gene encoding Myt1 revealed that it is most similar to kinases in the Wee1 family (Fig. 1B). The kinase domain of Myt1 has a similar degree of sequence similarity with all members of this family, ranging from

Division of Biology 216-76, Howard Hughes Medical Institute, California Institute of Technology, Pasadena, CA 91125, USA.

*To whom correspondence should be addressed.

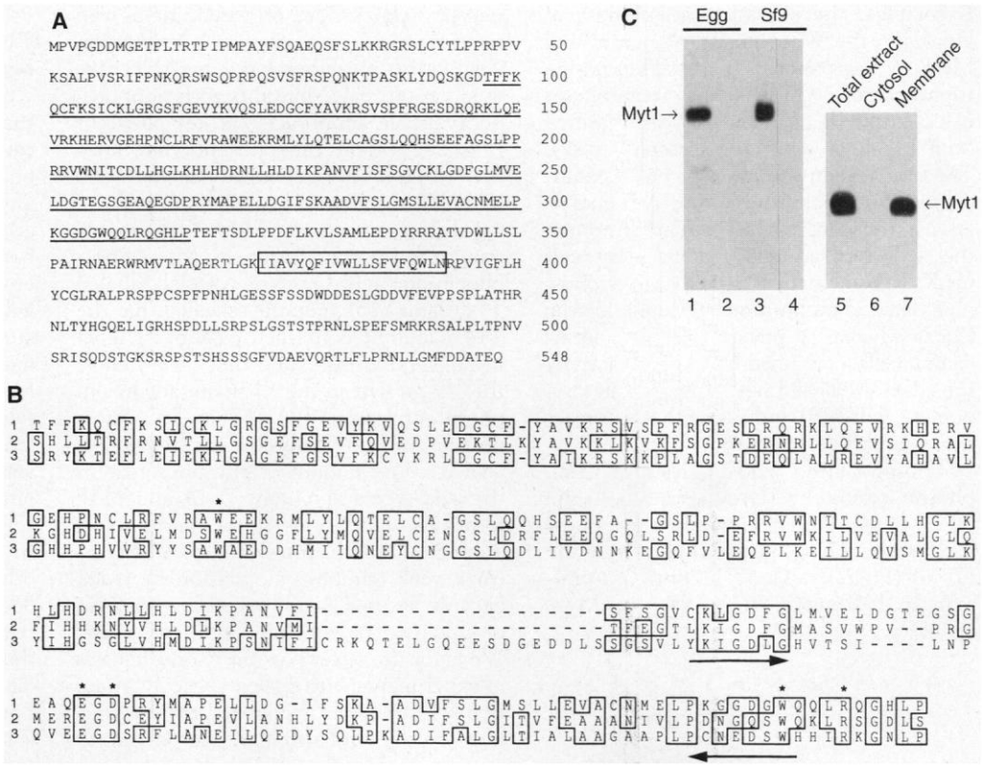

Fig. 1. Myt1, a membrane-associated member of the Wee1 kinase family. (**A**) Predicted amino acid sequence of Myt1 (*15, 19*). The nucleotide sequence of the Myt1 cDNA (GenBank accession number U28931) contains a predicted open reading frame of 548 amino acids which is preceded by two in-frame termination codons. The catalytic domain (underlined) and a putative transmembrane segment (boxed) are indicated. (**B**) Alignment of the catalytic domains from Myt1 (row 1), *S. pombe* Wee1 (row 2, residues 560 to 781), and *Xenopus* Wee1 (row 3, residues 210 to 443) was performed as described (*4*). Amino acids that are conserved in all known members of the Wee1 family, but not in other protein kinases, are designated with asterisks. Arrows indicate regions that were used to design degenerate PCR primers. (**C**) (Left panel) A *Xenopus* interphase egg extract was immunoprecipitated with antibodies to Myt1 (anti-Myt1) (lane 1) or control (lane 2) antibodies (*18*). Recombinant Myt1 was purified from infected Sf9 cells (lane 3), or a control mock preparation was prepared from uninfected cells (lane 4) as described (*17*). Then, all of these preparations were immunoblotted with anti-Myt1. (Right panel) Total interphase egg extract (lane 5) or the cytosol (lane 6) and membrane (lane 7) fractions of the extract (*4*) were subjected to immunoprecipitation with anti-Myt1 and then immunoblotted with anti-Myt1.

40% identical residues for *S. pombe* Wee1 to 35% for *S. pombe* Mik1 (*3*). The kinase domain of Myt1 has 39% identical residues to the previously identified *Xenopus* Wee1 homolog, whereas *Xenopus* and human Wee1 share 72% identical residues in this region (*4*). This suggests that Myt1 represents a distinct member of the Wee1 family rather than a closely related isoform.

Another distinguishing characteristic of Myt1 is that, unlike other known Wee1 kinases, it contains a potential transmembrane segment, raising the possibility that Myt1 might be an integral membrane protein. This segment is located outside the kinase domain and consists of a stretch of 20 hydrophobic or uncharged amino acids flanked on both ends by a basic residue (lysine or arginine). To examine the subcellular localization of the Myt1 protein, we fractionated *Xenopus* egg extracts into cytosol and membrane fractions by ultracentrifugation. Subsequently, we washed the membrane fraction with a buffer containing a high concentration of salt to remove weakly associated proteins. After immunoprecipitation and immunoblotting with antibodies to Myt1 (anti-Myt1), nearly all of the Myt1 protein was recovered in the washed membrane fraction, whereas essentially none was found in the cytosol (Fig. 1C). This distribution was observed with both interphase and mitotic extracts (*8*). In contrast, more than 90% of *Xenopus* Wee1 resides in the egg cytosol fraction (*4*). Thus, unlike Wee1, Myt1 appears to be a membrane-associated protein. Because the catalytic domain of Myt1 would presumably reside in the cytosol, Myt1 may be a type II membrane protein with its transmembrane segment serving as an uncleaved, internal signal sequence.

To examine the enzymatic properties of Myt1, we produced a histidine-tagged version of the protein in a baculoviral expression system (Fig. 1C). We asked whether Myt1 would phosphorylate a Cdc2–cyclin

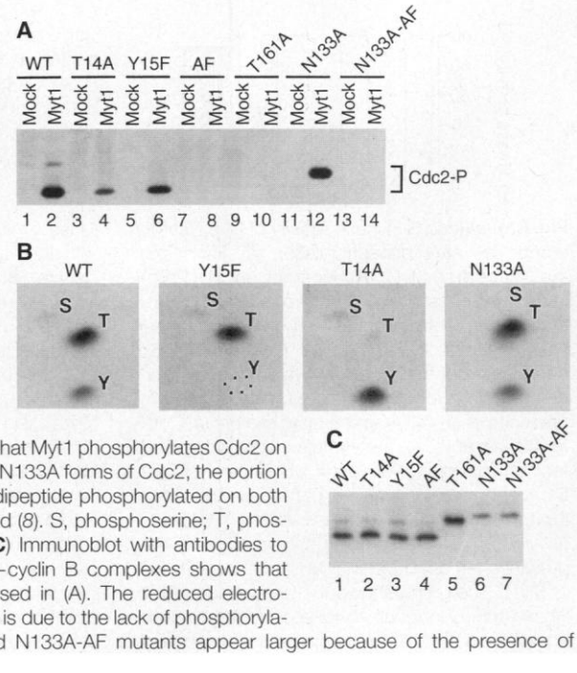

Fig. 2. Phosphorylation of Cdc2 on both Thr[14] and Tyr[15] by Myt1. (**A**) Recombinant Myt1 protein from Sf9 cells (even lanes) or a control mock preparation from uninfected cells (odd lanes) were incubated with purified Cdc2–cyclin B1 complexes containing the wild-type (WT) or indicated mutant forms of *Xenopus* Cdc2 (*9*) in the presence of [γ-^{32}P]ATP (*20*) (see text for explanation of mutant designations). After 15 min at 22°C, samples were processed for autoradiography. Cdc2-P, phosphorylated Cdc2; AF double mutant T14A,Y15F; N133A-AF, triple mutant T14A,Y15F,N133A. (**B**) Phosphoamino acid analysis (*21*) of the indicated samples from (A) shows that Myt1 phosphorylates Cdc2 on Thr[14] and Tyr[15]. For the wild-type and N133A forms of Cdc2, the portion of the autoradiogram containing the dipeptide phosphorylated on both Thr[14] and Tyr[15] has not been depicted (*8*). S, phosphoserine; T, phosphothreonine; Y, phosphotyrosine. (**C**) Immunoblot with antibodies to *Xenopus* Cdc2 of the various Cdc2–cyclin B complexes shows that similar amounts of substrate were used in (A). The reduced electrophoretic mobility of the T161A mutant is due to the lack of phosphorylation on Thr[161]. Both the N133A and N133A-AF mutants appear larger because of the presence of a hemagglutinin tag.

B complex, the physiological substrate of kinases in the Wee1 family. We incubated Myt1 in the presence of [γ-^{32}P]adenosine triphosphate (ATP) and a recombinant Cdc2–cyclin B complex that was purified from baculovirus-infected insect cells (9). The Cdc2-cyclin complex was prepared under conditions that allow the phosphorylation of the Cdc2 subunit on Thr^{161} through the action of an endogenous insect cell CAK. Recombinant Myt1 efficiently phosphorylated cyclin-associated, wild-type Cdc2, whereas a preparation from uninfected cells contained no kinase activity (Fig. 2A). Myt1 did not phosphorylate monomeric Cdc2 (8), indicating that this reaction is cyclin-dependent.

Phosphoamino acid analysis of Cdc2 phosphorylated by Myt1 revealed that the ^{32}P was distributed between both phosphotyrosine (20%) and phosphothreonine (77%) (Fig. 2B). Thus, in contrast to human and *Xenopus* Wee1 (4, 5), Myt1 phosphorylates Cdc2 on threonine as well as on tyrosine. To assess which residues on Cdc2 were phosphorylated by Myt1, we used various Cdc2 mutants with nonphosphorylatable amino acids at key positions (Fig. 2A). Myt1 can phosphorylate both the T14A (Thr^{14} changed to Ala) and Y15F (Tyr^{15} changed to Phe) mutants of Cdc2. In contrast, the T14A,Y15F double mutant was not a substrate for Myt1. Phosphoamino acid analysis of ^{32}P-labeled T14A and Y15F mutants revealed that the T14A mutant contained 89% of its label in phosphotyrosine, and that nearly all of the ^{32}P present in the Y15F mutant was in phosphothreonine (96%) (Fig. 2B). Phosphoamino acid analysis consistently revealed a low amount of phosphoserine in the wild-type and mutant T14A and Y15F forms of Cdc2. This serine phosphorylation could result from activity of Myt1 or from weak autophosphorylation by Cdc2 because we used a catalytically active form of Cdc2 as the substrate in these assays. We favor the latter possibility on the basis of experiments with the catalytically inactive N133A (Asn^{133} changed to Ala) mutant of Cdc2. In particular, phosphoamino acid analysis of the N133A mutant phosphorylated by Myt1 (Fig. 2, A and B) revealed the presence of mainly phosphothreonine (75%) and phosphotyrosine (24%), but essentially no phosphoserine (<0.7%). As expected, the triple mutant T14A,Y15F,N133A was not a substrate for Myt1 (Fig. 2A).

Taken together, these results indicate that Myt1 is a dual-specificity kinase that can efficiently phosphorylate Cdc2 on both Thr^{14} and Tyr^{15}. We do not observe any obligatory order to the phosphorylation of Cdc2 at these two sites, because both the T14A and Y15F single mutants of Cdc2 are substrates for Myt1. However, wild-type Cdc2 appears to be phosphorylated more efficiently than either single mutant (8). Unlike *Xenopus* Wee1 (4), Myt1 appears to require prior phosphorylation of Cdc2 on Thr^{161} in order for Cdc2 to be a substrate (8). Consistent with this observation, Myt1 did not phosphorylate the T161A mutant of Cdc2 (Fig. 2A) on either tyrosine or threonine. In addition, like Mik1 (10), but unlike other Wee1 homologs (4, 5, 11), Myt1 does not have detectable autophosphorylation activity (8). Finally, we observed that Myt1 itself is a substrate for the active Cdc2–cyclin B complex (8), but the functional significance of this phosphorylation is not known at present.

We examined whether the kinase activity of Cdc2 could be altered by Myt1-mediated phosphorylation. We incubated wild-type and mutant forms of Cdc2 with Myt1 in the presence of an ATP-regener-

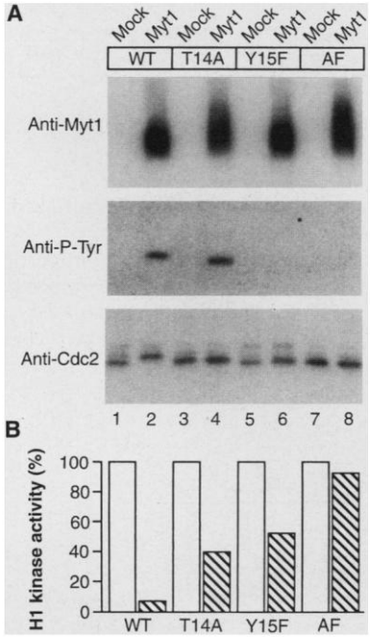

Fig. 3. Reduced H1 kinase activity of Cdc2-cyclin complexes after phosphorylation on Thr^{14} and Tyr^{15} or both by Myt1. (**A**) Recombinant Myt1 protein from Sf9 cells (even lanes) or a control preparation (mock) from uninfected cells (odd lanes) were incubated with purified Cdc2–cyclin B1 complexes containing the wild-type (WT) or indicated mutant forms of *Xenopus* Cdc2 (9) in the presence of an ATP-regenerating system (20). After 30 min at 22°C, the samples were processed for immunoblotting with anti-Myt1 (top panel), anti-phosphotyrosine (middle panel), or anti-Cdc2 (bottom panel). (**B**) Cdc2-associated H1 kinase activity (22) of the samples shown in (A) in the presence (stripped bars) or absence (open bars) of Myt1. The graph shows the percentage of H1 kinase activity (normalized for each mutant; 100% equals the activity of the sample in the absence of Myt1).

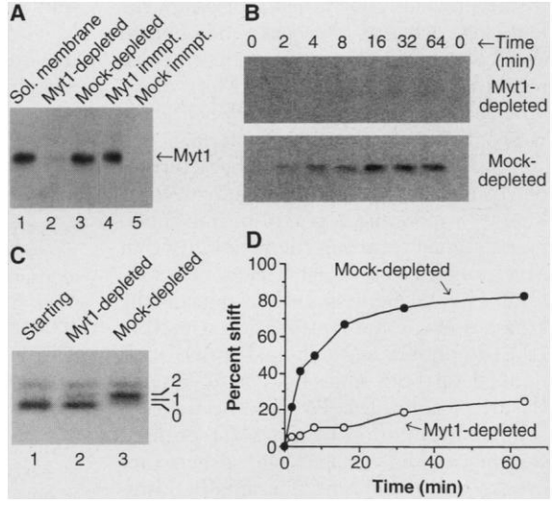

Fig. 4. Myt1 is a major Cdc2-specific tyrosine and threonine kinase in the membrane fraction of *Xenopus* egg extracts. (**A**) The membrane fraction of an interphase *Xenopus* egg extract was solubilized with Triton X-100 (lane 1) and either treated with anti-Myt1 (lanes 2 and 4) or with control antibodies (lanes 3 and 5). Protein A beads were added, incubated, and removed along with associated proteins as described (23). The solubilized membrane fraction (lane 1), depleted supernatants (lanes 2 and 3), and isolated beads (lanes 4 and 5) were immunoblotted with anti-Myt1. Immpt., immunoprecipitate. (**B**) Reduced Cdc2-specific tyrosine kinase activity after removal of Myt1. These Myt1-depleted or control extracts were incubated at 22°C with a purified Cdc2–cyclin B1 complex (9) in the presence of 2 mM ATP, 10 mM phosphocreatine, creatine kinase (100 μg/ml), 10 mM $MgCl_2$, and 1 mM vanadate. Samples were taken at the indicated times and immunoblotted with antibodies to phosphotyrosine. (**C**) Reduction of Cdc2-specific threonine and tyrosine kinase activities after removal of Myt1. The Myt1-depleted or control extracts were incubated as described in (B) except the Cdc2 subunit was labeled with ^{35}S during its synthesis (9). After a 30-min incubation, samples were processed for autoradiography. In lane 1, the starting complex was loaded for reference. The phosphorylated forms of Cdc2 (12) are indicated: 0, unshifted Cdc2; 1, partially shifted Cdc2 after phosphorylation on either Thr^{14} or Tyr^{15}; or 2, fully shifted Cdc2 after phosphorylation on both Thr^{14} and Tyr^{15}. (**D**) Time course of an experiment similar to (C), except that the Cdc2 was labled with ^{32}P on Thr^{161} (24) before it was added to either the Myt1-depleted or control extracts as described in (B). At the indicated times, samples were processed for autoradiography (25). The graph shows the percentage of Cdc2 that is phosphorylated on both Thr^{14} and Tyr^{15}.

ating system and subsequently measured the Cdc2-associated histone H1 kinase activity (Fig. 3). In these experiments, phosphorylation of Cdc2 was assessed either by immunoblotting with antibodies to phosphotyrosine or by observing the reduced mobility of modified Cdc2 during gel electrophoresis. The wild-type Cdc2 protein that had been treated with Myt1 reacted strongly with antibodies to phosphotyrosine and displayed the characteristic double shift (*12*) in SDS-polyacrylamide gels indicative of phosphorylation on both Thr^{14} and Tyr^{15} (Fig. 3A). The same analysis showed that the T14A and Y15F mutants are single-shifted as a result of phosphorylation at only one site. Treatment of wild-type Cdc2 with Myt1 caused a 90% reduction in its H1 kinase activity. Similarly, phosphorylation of both the T14A and Y15F mutants by Myt1 resulted in a large reduction in activity (60 and 50%, respectively). As expected, the T14A,Y15F double mutant of Cdc2 was neither phosphorylated nor inactivated by Myt1 (Fig. 3, A and B). Collectively, these experiments indicate that phosphorylation of Thr^{14} and Tyr^{15} or both by Myt1 leads to a substantial reduction in the catalytic activity of Cdc2.

The membrane fraction from *Xenopus* egg extracts possesses both Thr^{14}- and Tyr^{15}-specific kinase activities, whereas the cytosol fraction contains only the tyrosine-specific kinase (*7*). To determine whether Myt1 can account for a substantial portion of the Cdc2-specific inhibitory kinase activity found in *Xenopus* egg membranes, we carried out a series of immunodepletion studies with antibodies to the last 12 carboxyl residues of Myt1 (Fig. 4). Proteins from the detergent-solubilized membrane fraction from *Xenopus* eggs were immunoprecipitated with either anti-Myt1 or control antibodies. This immunodepletion with anti-Myt1 removed ~85% of the Myt1 protein (Fig. 4A). We measured the Cdc2-specific kinase activities in the Myt1-depleted or control extracts by adding a Cdc2-cyclin complex and then examining either the phosphotyrosine content of Cdc2 with antibodies to phosphotyrosine or the phosphorylation-dependent retardation of radiolabeled Cdc2 during gel electrophoresis. The tyrosine phosphorylation of Cdc2 was dramatically reduced in the Myt1-depleted extract (Fig. 4B). Similarly, using either ^{35}S- or ^{32}P-labeled Cdc2 as the substrate, we observed that the control extract shifted ~80% of the Cdc2 to its Thr^{14}-Tyr^{15} doubly phosphorylated form (*12*), whereas the Myt1-depleted extract phosphorylated only about 20% of the substrate (Fig. 4, C and D). The immunoprecipitated Myt1 protein efficiently phosphorylated Cdc2 in both assays (*8*). Taken together, these experiments suggest that Myt1 is a predominant Cdc2-specific inhibitory kinase in *Xenopus* egg membranes. Moreover, because all of the Thr^{14}-directed activity resides in the membrane fraction, Myt1 appears to be a major Thr^{14}-specific kinase in *Xenopus* eggs.

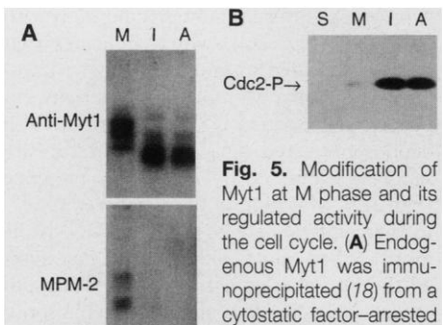

Fig. 5. Modification of Myt1 at M phase and its regulated activity during the cell cycle. (**A**) Endogenous Myt1 was immunoprecipitated (*18*) from a cytostatic factor–arrested *Xenopus* egg extract (lane M), an interphase extract (lane I), or an S phase–blocked extract that had been treated with aphidicolin (50 μg/ml) in the presence of sperm nuclei (1000 per microliter) (lane A). These samples were immunoblotted with anti-Myt1 (top panel) or monoclonal antibody MPM-2 (bottom panel). (**B**) The kinase activity of the various forms of immunoprecipitated Myt1 was measured as described in Fig. 2 with the N133A form of Cdc2 as the substrate (S). Lane S depicts a control assay without added Myt1 protein.

The Wee1 kinase from *Xenopus* and humans is highly regulated during the cell cycle (*4*, *6*). In particular, *Xenopus* Wee1 is active during interphase but shows greatly reduced activity at mitosis as a result of extensive phosphorylation by two inhibitory kinases. To examine whether Myt1 is regulated during the cell cycle, we immunoprecipitated endogenous Myt1 from either M phase or interphase *Xenopus* egg extracts and measured its Cdc2-specific kinase activity. We prepared two types of interphase extracts: one that was arrested in interphase with the replication inhibitor aphidicolin (*13*) and another that contained no cell cycle inhibitor. Equivalent amounts of Myt1 protein were immunoprecipitated from the various extracts. However, the M phase form of Myt1 was clearly modified as indicated by a substantially reduced electrophoretic mobility (Fig. 5A). At least a portion of this modification appears to be phosphorylation, because the M phase, but not interphase, form of Myt1 reacts well with the mitotic phosphoprotein monoclonal antibody MPM-2 (Fig. 5A). This antibody specifically recognizes a phosphorylated epitope found on various mitotic proteins (*14*). Finally, we examined the Cdc2-specific kinase activity of the various forms of Myt1 (Fig. 5B). The M phase form was about one-fifth as active as the Myt1 protein from either type of interphase extract. Moreover, like *Xenopus* Wee1 (*4*), the activity of Myt1 was similar during interphase whether or not the replication checkpoint had been activated by aphidicolin. Similar results were obtained if either the T14A or Y15F form of Cdc2 was used (*8*). These experiments indicate that Myt1 activity is substantially decreased at mitosis when Cdc2 must remain dephosphorylated on both Thr^{14} and Tyr^{15}.

In conclusion, we have identified Myt1, a distinct member of the Wee1 family that collaborates with Wee1 by phosphorylating Cdc2 on Thr^{14} in addition to Tyr^{15}. Collectively, the inhibitory Wee1 and Myt1 kinases may ensure that Cdc2 at various locations throughout the cell becomes activated only at the G_2-M transition.

REFERENCES AND NOTES

1. T. R. Coleman and W. G. Dunphy, *Curr. Opin. Cell Biol.* **6**, 877 (1994); W. G. Dunphy, *Trends Cell Biol.* **4**, 202 (1994); R. W. King, P. K. Jackson, M. W. Kirschner, *Cell* **79**, 563 (1994); D. O. Morgan, *Nature* **374**, 131 (1995)
2. P. Russell and P. Nurse, *Cell* **49**, 559 (1987).
3. R. N. Booher, R. J. Deshaies, M. W. Kirschner, *EMBO J.* **12**, 3417 (1993); M. Igarashi, A. Nagata, S. Jinno, K. Suto, H. Okayama, *Nature* **353**, 80 (1991); K. Lundgren *et al.*, *Cell* **64**, 1111 (1991); GenBank accession number Z36752 (*Caenorhabditis elegans*); GenBank accession number U25693 (*Emericella nidulans*); GenBank accession number D30743 (*Mus musculus*).
4. P. R. Mueller, T. R. Coleman, W. G. Dunphy, *Mol. Biol. Cell* **6**, 119 (1995).
5. C. H. McGowan and P. Russell, *EMBO J.* **12**, 75 (1993); L. L. Parker and H. Piwnica-Worms, *Science* **257**, 1955 (1992).
6. C. H. McGowan and P. Russell, *EMBO J.* **14**, 2166 (1995); N. Watanabe, M. Broome, T. Hunter, *ibid.*, p. 1878.
7. S. Atherton-Fessler *et al.*, *Mol. Biol. Cell* **5**, 989 (1994); S. Kornbluth, B. Sebastian, T. Hunter, J. Newport, *ibid.*, p. 273.
8. P. R. Mueller and W. G. Dunphy, unpublished results.
9. A. Kumagai and W. G. Dunphy, *Mol. Biol. Cell* **6**, 199 (1995).
10. M. S. Lee, T. Enoch, H. Piwnica-Worms, *J. Biol. Chem.* **269**, 30530 (1994).
11. C. Featherstone and P. Russell, *Nature* **349**, 808 (1991).
12. B. A. Edgar, F. Sprenger, R. J. Duronio, P. Leopold, P. H. O'Farrell, *Genes Dev.* **8**, 440 (1994); M. J. Solomon, T. Lee, M. W. Kirschner, *Mol. Biol. Cell* **3**, 13 (1992).
13. M. Dasso and J. W. Newport, *Cell* **61**, 811 (1990).
14. J. Kuang, C. L. Ashorn, M. Gonzalez-Kuyvenhoven, J. E. Penkala, *Mol. Biol. Cell* **5**, 135 (1994).
15. Abbreviations for the amino acid residues are as follows: A, Ala; C, Cys; D, Asp; E, Glu; F, Phe; G, Gly; H, His; I, Ile; K, Lys; L, Leu; M, Met; N, Asn; P, Pro; Q, Gln; R, Arg; S, Ser; T, Thr; V, Val; W, Trp; and Y, Tyr.
16. T. R. Coleman, Z. Tang, W. G. Dunphy, *Cell* **72**, 919 (1993).
17. A baculovirus expression vector (pVL-HIS-XeMyt1) encoding a histidine-tagged version of Myt1 was prepared with PCR to convert the initiation codon to an Nde I site as described (*4*). The 5′ primer was CGGCATATGCCTGTTCCAGGGGATG and the 3′ primer was CAAGGCTTTGCACCTTGTATACCTC. Recombinant Myt1 protein was produced in adherent Sf9 insect cells and bound to nickel–iminidoacetic acid beads (*9*). The Myt1-containing beads were then washed four times in lysis buffer [10 mM Hepes-NaOH (pH 7.4), 150 mM NaCl, 5 mM EGTA, 0.5% Triton X-100, 0.2 mM phenylmethylsulfonyl fluoride, and protease inhibitor mix (10 μg each of pepstatin, chymostatin, and leupeptin per milliliter)] and then

washed four times in wash buffer (lysis buffer without EGTA and Triton X-100). Recombinant Myt1 protein was eluted from the beads with 150 mM imidazole in wash buffer, frozen in liquid nitrogen, and stored at −80°C. A mock preparation was prepared in the same manner from uninfected Sf9 cells.
18. Rabbit antibodies to the COOH-terminal end of Myt1 (CNLLGMFDDATEQ) (*15*) were affinity-purified as described (*16*). Affinity-purified rabbit antibodies to mouse immunoglobulin G (Cappel) served in control experiments. All other antibodies were described previously (*9*). Endogenous Myt1 was immunoprecipitated from *Xenopus* egg extracts with anti-Myt1 as described (*4*) except that 0.5% Triton X-100 replaced NP-40.
19. An internal fragment of the Myt1 cDNA was amplified by PCR as described (*4*) except that the annealing temperature was 45°C for the first five cycles and 55°C for the remaining 30 cycles. The 5′ and 3′ primers were CGGGGTACC(C/T)T(A/G)AA(I/C)(C/T/A)TIGGIGA(T/C)(T/C)T(I/C)GG and TCCCCCGGGTGCCAI(T/G/C)II(T/A)(C/G)ICC(G/A)TT(I/C)(C/T)(G/T/C)(I/C)GG, respectively. This reaction yielded a 221–base pair fragment that was used to isolate a full-length Myt1 cDNA from a *Xenopus* oocyte library as described (*4*).
20. The conditions for in vitro kinase assays of Myt1 were as described (*4*) for Wee1 except that 0.05 % Triton X-100 was added.
21. W. J. Boyle, P. Van Der Geer, T. Hunter, *Methods Enzymol.* **201**, 110 (1991).
22. W. G. Dunphy and J. W. Newport, *Cell* **58**, 181 (1989).
23. An interphase extract from *Xenopus* eggs was made in the presence of cycloheximide (100 μg/ml) as described (*4*). All subsequent steps were done on ice or at 4°C. The extract was diluted with two volumes of DB [20 mM Hepes (pH 7.6), 100 mM NaCl, 5 mM NaF, 1 mM $Na_4P_2O_7$, 1 mM dithiothreitol, and protease inhibitor mix (*17*)] and centrifuged at 260,000*g* for 1 hour. The membrane fraction was resupended in three volumes of DB containing 500 mM NaCl and recentrifuged for 30 min. This salt-washed membrane was resuspended in three volumes of DB containing 0.5 % Triton X-100, rotated for 20 min, and recentrifuged for 30 min. The resulting supernatant (the solubilized membrane fraction) was either frozen for later use or immediately subjected to immunodepletion. For this purpose, the solubilized membrane fraction was incubated with 20 μg of either anti-Myt1 or control antibodies per milliliter and bound to protein A beads as described (*18*). After this incubation, the beads were removed by centrifugation to yield Myt1-depleted or control-depleted supernatant. These depleted extracts were frozen in liquid nitrogen and stored at −80°C.
24. Cdc2 was labeled on Thr^{161} with [γ-^{32}P]ATP as described (*9*) except the reaction contained 500 μM nonradioactive ATP.
25. Immunoblotting was performed as described (*4*). Quantification was performed with a PhosphorImager (Molecular Dynamics).
26. We are grateful to D. Morgan (University of California, San Francisco) for supplying the baculovirus transfer vector, M. Solomon (Yale University) for providing Cdc2 mutant plasmids, J. Kuang (M. D. Anderson Cancer Center) for supplying MPM-2 antibodies, and B. Wold and members of the W.G.D. group for critical reading of this manuscript. Supported by grants from NIH, Lucille P. Markey Charitable Trust, and NSF. P.R.M. and T.R.C. were supported by fellowships from the Helen Hay Whitney Foundation and NIH (National Research Service Awards), respectively. P.R.M. is an associate and W.G.D. is an investigator at the Howard Hughes Medical Institute.

29 June 1995; accepted 6 September 1995

Dephosphorylation of Cdk2 Thr^{160} by the Cyclin-Dependent Kinase–Interacting Phosphatase KAP in the Absence of Cyclin

Randy Y. C. Poon and Tony Hunter

The activation of cyclin-dependent kinases (CDKs) requires the phosphorylation of a conserved threonine (Thr^{160} in Cdk2) by CDK-activating kinase (CAK). Human KAP (also called Cdi1), a CDK-associated phosphatase, was shown to dephosphorylate Thr^{160} in human Cdk2. KAP was unable to dephosphorylate Tyr^{15} and only dephosphorylated Thr^{160} in native monomeric Cdk2. The binding of cyclin A to Cdk2 inhibited the dephosphorylation of Thr^{160} by KAP but did not preclude the binding of KAP to the cyclin A–Cdk2 complex. Moreover, the dephosphorylation of Thr^{160} by KAP prevented Cdk2 kinase activity upon subsequent association with cyclin A. These results suggest that KAP binds to Cdk2 and dephosphorylates Thr^{160} when the associated cyclin subunit is degraded or dissociates.

CDKs are key regulators of cell cycle progression (*1*, *2*). Activation of Cdk2 requires cyclin binding and phosphorylation of Thr^{160} by CAK (*3*). To investigate whether the dephosphorylation of Cdk2 Thr^{160} is affected by binding to cyclin, we sought a Cdk2 substrate that could be phosphorylated by CAK to the same extent with or without the cyclin subunit. A bacterially expressed glutathione-S-transferase (GST)–Cdk2 fusion protein could be phosphorylated by CAK without binding to cyclin (Fig. 1A), although catalytic activity requires both Thr^{160} phosphorylation and cyclin A association (*4*). When the GST domain was cleaved with thrombin, the monomeric Cdk2 was phosphorylated by CAK weakly, but phosphorylation was greatly enhanced by binding to cyclin A (Fig. 1B). To generate monomeric and cyclin-complexed Cdk2 substrates in order to assay Thr^{160} phosphatase activity, we therefore first phosphorylated GST-Cdk2 with CAK before cleaving with thrombin. Half of the cleaved Thr^{160}-phosphorylated Cdk2 was incubated with buffer and the other half with purified cyclin A. Monomeric Thr^{160}-phosphorylated Cdk2 was rapidly dephosphorylated when it was added to an EDTA-treated extract from *Xenopus* eggs (Fig. 1C). In contrast, the Thr^{160} phosphate in the cyclin A–Cdk2 complex was relatively stable. Immunoblotting showed that the loss of labeling in Cdk2 was not the result of protein degradation. Similar results were obtained with a HeLa cell extract (see below). Thus, vertebrate cell extracts contain an activity that dephosphorylates Thr^{160} preferentially when Cdk2 is monomeric.

The physiological Thr^{160} phosphatase is unknown (*5*). Protein phosphatase 2A (PP2A) can dephosphorylate Thr^{160} in vitro, but this occurs in the presence or absence of cyclin (see below). The CDK-associated phosphatase KAP, a dual-specificity phosphatase (*6*) that was identified as a protein that interacts with Cdk2 and Cdc2, is a plausible candidate Thr^{160} phosphatase. KAP is related to MKP-1 and PAC1, dual-specificity phosphatases that dephosphorylate the activating threonine and tyrosine phosphates in the ERK1 and ERK2 members of the mitogen-activated protein (MAP) kinase family, which lie in the catalytic domain activation loop in a position similar to that of Thr^{160} in Cdk2 (*7*). We therefore investigated whether KAP could dephosphorylate Cdk2 Thr^{160}. KAP that was immunoprecipitated with affinity-purified antibodies to KAP (anti-KAP) from HeLa cell extracts (Fig. 2A) was found to dephosphorylate monomeric Thr^{160}-phosphorylated Cdk2, but not the cyclin A–Cdk2 complex (Fig. 2B). These results were consistent with the observed dephosphorylation of Cdk2 Thr^{160} by cell extracts (Fig. 1C). The Thr^{160} dephosphorylation activity in a HeLa cell extract was reduced after immunoprecipitation with anti-KAP (Fig. 2C), which indicates that KAP constituted a significant Thr^{160} phosphatase activity. Moreover, a bacterially expressed and purified GST-KAP protein also dephosphorylated Cdk2 Thr^{160} in the absence of cyclin A, but not in its presence (Fig. 2D). Mutation of the conserved Cys^{140} in the catalytic core of KAP (HCXXXXGR motif) (*8*) to Ser (C140S), which inactivated the phosphatase activity of KAP toward model substrates (*6*), abolished dephosphorylation of Cdk2 Thr^{160} (Fig. 2D). The dephosphorylation of Cdk2 by KAP did not depend on the kinase activity of Cdk2, because the reaction contained no Mg^{2+}–adenosine triphosphate and because a catalytically inactive mutant of Cdk2 in which Lys^{33} was changed to Arg (K33R) (*4*) was efficiently dephosphorylated (*9*). Similar results were obtained with a hexahistidine-tagged cyclin A or a protein A–tagged KAP

Molecular Biology and Virology Laboratory, Salk Institute for Biological Studies, 10100 North Torrey Pines Road, La Jolla, CA 92037–1099, USA.